SEDIMENTOLOGY

The exceptional sediment load of fine-grained dispersal systems: Example of the Yellow River, China

Hongbo Ma,[1]* Jeffrey A. Nittrouer,[1] Kensuke Naito,[2] Xudong Fu,[3] Yuanfeng Zhang,[4] Andrew J. Moodie,[1] Yuanjian Wang,[4] Baosheng Wu,[3] Gary Parker[2,5]

Sedimentary dispersal systems with fine-grained beds are common, yet the physics of sediment movement within them remains poorly constrained. We analyze sediment transport data for the best-documented, fine-grained river worldwide, the Huanghe (Yellow River) of China, where sediment flux is underpredicted by an order of magnitude according to well-accepted sediment transport relations. Our theoretical framework, bolstered by field observations, demonstrates that the Huanghe tends toward upper-stage plane bed, yielding minimal form drag, thus markedly enhancing sediment transport efficiency. We present a sediment transport formulation applicable to all river systems with silt to coarse-sand beds. This formulation demonstrates a remarkably sensitive dependence on grain size within a certain narrow range and therefore has special relevance to silt-sand fluvial systems, particularly those affected by dams.

INTRODUCTION

Sedimentary environments that have fine-grained beds consisting of silt and very fine sand (median grain size range, 15 to 150 μm) are common on Earth and extraplanetary surfaces, with examples including fluvial, deltaic, coastal, and marine settings, as well as subglacial transport systems (Fig. 1A) (*1*–*7*). These settings are morphologically active (*8*), and many have significant relevance to human well-being. For example, low-lying deltaic coastal regions, threatened by ocean storms and rising sea levels, provide living space for approximately 40% of world's population (*9*, *10*). To bolster the predictive capabilities of models that assess the evolution and vulnerability of these regions, it is necessary to evaluate the physics of fine-grained dispersal systems (FGDS). However, to date, the mechanics of fine-grained sediment transport remain poorly constrained because of a paucity of field-scale data necessary to properly inform predictive algorithms. In turn, this is due to the difficulty in measuring quasi-equilibrium transport conditions for FGDS, whereby the observational window required to establish approximately steady and uniform flow is rarely achieved. Although flume experiments using fine-grained sediment have yielded sediment transport data (*11*–*16*), the formulae developed from these studies have proven inadequate for predictions at field-scale without significant modifications (*17*–*19*). Therefore, no physical formulae that claim the ability to predict sediment transport for FGDS show convincing and consistent agreement with both flume and field data (*18*). In contrast, coarser sediment dispersal systems (for example, sand to gravel) can be characterized by numerous physically based and properly validated sediment transport relations applicable to a range of environments (Fig. 1A).

The lower Huanghe (Yellow River) of China (fig. S1) presents an exceptional opportunity to develop a physics-based sediment transport model applicable to FGDS. It is the most robustly measured fine-grained river system in the world (*20*), and the spatiotemporal resolution of the measurements is adequate to document quasi-equilibrium sediment transport conditions. We use this rich database from the Huanghe to inform a new model of fine-grained sediment transport that, because it is grounded in basic physics, is applicable to other dispersal systems as well. There are cultural and engineering perspectives underlining the value of using the lower Huanghe to develop a sediment transport formula: This region is the "cradle" of Chinese civilization but is also known as the "sorrow" of the Chinese people because of rapid channel platform change produced by an exceptionally high sediment load (*21*, *22*). The Huanghe traverses 800 km of the North China Plain and, until recently, delivered approximately 1 billion tons/year of sediment to the Bohai Sea with as little as 49 billion tons of water. The river has maintained one of the largest sediment loads worldwide, with a volumetric sediment concentration exceeding large lowland rivers by an order of magnitude (*23*–*25*). This sediment, derived from the denudation of friable Loess Plateau soil, has constructed over 30,000 km^2 of land on the North China Plain over the past several millennia (fig. S1) (*26*). The river and floodplain system perpetually teeters on the brink of societal sustainability. Seven major avulsions in the past 2000 years have each disrupted 8 to 14 million people, collectively inundating approximately 250,000 km^2 of floodplain (*27*). In the past several centuries, there have been greater than 1000 levee breaches (*28*), and the recurrence interval of channel avulsions is 7 to 14 years (*29*). Over the past century, sediment deposited within the heavily diked plain has produced riverbed superelevation of as much as 10 m, jeopardizing the 88 million inhabitants living on the floodplain. Over the past several decades, Chinese engineers have stabilized the river by building levees and dikes to constrain channel migration (*20*). Meanwhile, the Xiaolangdi Dam and Reservoir (fig. S1), which was finished in 2002, stores sediment derived from the Loess Plateau while releasing sediment-depleted water into to the lower Huanghe in an effort to reduce bed elevation. These water-release events have occurred annually for the past 15 years as part of the government's Water and Sediment Regulation Season (WSRS). The effectiveness and impact of Xiaolangdi Dam and WSRS in sustaining the lower Huanghe require quantitative evaluation (*30*–*32*). Developing and implementing engineering measures to ensure future safety of neighboring inhabitants render critical the ability to accurately model sediment and water flux.

Here, we first show that the sediment loads in the Huanghe, based on 10 years of measurements, are an order of magnitude higher than is otherwise predicted by the well-accepted sediment transport formula. Second, this rich database is compiled and used to inform the development of a physically based theory, which, in turn, is validated with field surveys that measure the geometry of the channel bedforms. These efforts of combining a new theoretical framework and field observations yield the primary finding that the Huanghe tends toward upper-regime plane bed,

[1]Department of Earth Science, Rice University, Houston, TX 77251, USA. [2]Ven Te Chow Hydrosystems Laboratory, Department of Civil and Environmental Engineering, University of Illinois at Urbana-Champaign, Champaign, IL 61801, USA. [3]State Key Laboratory of Hydroscience and Engineering, Tsinghua University, Beijing 100084, P. R. China. [4]Yellow River Institute of Hydraulic Research, Zhengzhou, Henan 450000, P. R. China. [5]Department of Geology, University of Illinois at Urbana-Champaign, Champaign, IL 61801, USA.
*Corresponding author. Email: sediment@rice.edu

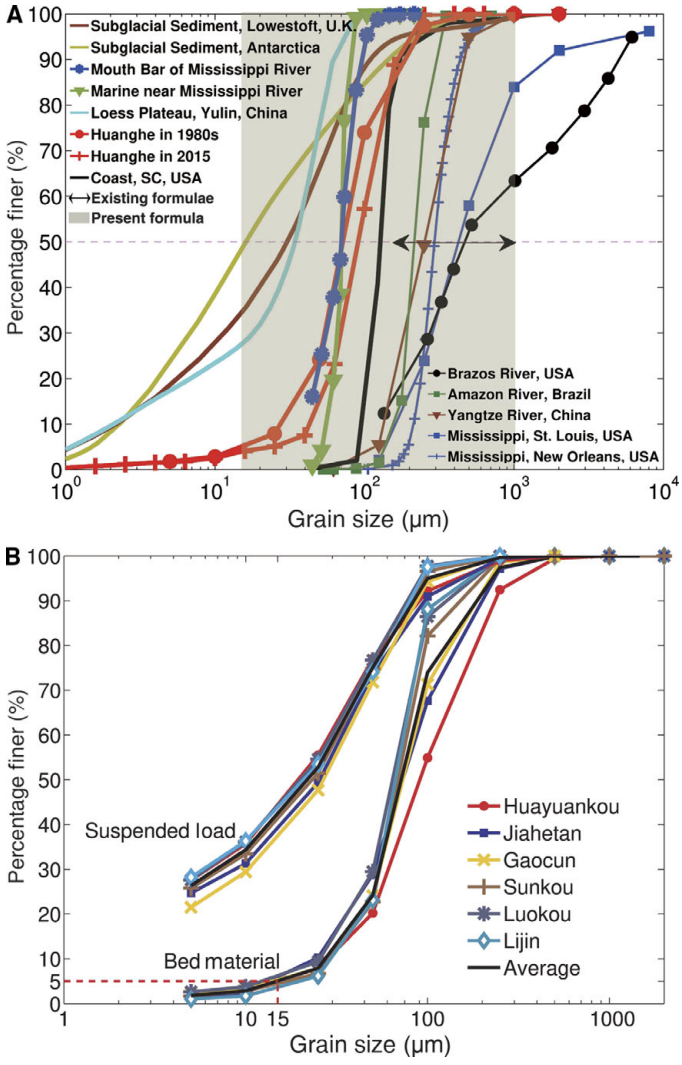

Fig. 1. GSDs of sediment from both silty and sandy dispersal environments. (**A**) Comparison of GSDs for a range of sedimentary environments, including the Huanghe, where median sediment size ranges from silt to fine sand. The left-right arrow indicates the grain size range for which standard, physics-based transport formulae have been previously designed. The light brown bar indicates the grain size range that the formula presented here accounts for silt and very fine sand. Note that many natural sediment transport systems fall in the silt to very-fine sand range, for which no unifying sediment transport relation exists. (**B**) GSDs of suspended sediment and bed material, sampled at six gauging stations on the lower Huanghe (see fig. S1 for the locations of the gauging stations).

so as to yield minimal form drag and thus markedly enhance sediment transport efficiency. Third, we present the unified sediment transport formulation that is applicable to all other river systems with channel beds possessing silt to coarse-sand sediment. This unified formulation demonstrates the remarkable sensitivity of sediment flux to sediment grain size within a certain narrow range. The results herein may be applied universally to assess fluvial responses to changing bed material size, which is particularly salient for systems impacted by dams.

THEORY AND RESULTS

Our starting point is the development of a generalized form of the Engelund-Hansen sediment transport theory (EH) (*33*), which is a widely validated sand-bed sediment transport relation and therefore provides the basis to compare the Huanghe to other sand-bed rivers. For example, Brownlie and Brooks (*17*) collected ~1000 sets of field and flume data, tested 13 sediment transport formulae, and determined that EH performed best. EH derives from basic physics (*33*); its dimensionless form reads $C_f q_s^* = \alpha_{EH} \tau^{*5/2}$, where $q_s^* = q_s/\sqrt{RgD^3}$ is the dimensionless sediment discharge, that is, the Einstein number [$q_s = HUC$ is the sediment discharge per unit width (H is the water depth; U is the average flow velocity; and C is the depth-flux–averaged volumetric sediment concentration); R is the sediment submerged specific gravity (1.65 for quartz); g is the gravitational acceleration; and D is the characteristic (nominal) diameter of bed sediment]; $C_f = gHS/U^2$ is the bed resistance coefficient (S is the channel bed slope); $\tau^* = HS/(RD)$ is the dimensionless bed shear stress under normal flow conditions, that is, the Shields number; and $\alpha_{EH} = 0.05$. See Materials and Methods concerning these definitions.

The bed material of the lower Huanghe consists of silt and very fine sand, with a median grain diameter (D_{50}) of ~70 μm (Fig. 1A). This is different from most lowland rivers, where median grain size usually exceeds 200 μm (*34*). The bed grain size of the lower Huanghe is far below the grain size range that existing formulae consider (Fig. 1A and table S1). Figure 2A shows that EH underpredicts sediment transport for the Huanghe by an order of magnitude. Nevertheless, because the EH formula is grounded in physics, it is possible to modify and adapt this relation to fine-grained sediment transport systems.

To do so, we use a quasi-equilibrium sediment transport database (see Materials and Methods for the data sources and collection procedures) pertaining to nonhyperconcentrated flow conditions recorded at six hydrological stations located between Huayuankou and Lijin (figs. S1 and S2). Along this stretch of river, the mean grain size distributions (GSDs) of both suspended load and bed material are relatively constant (Fig. 1B). As shown in Fig. 1B, there is a portion of the suspended load that is composed of particles smaller than what is found in appreciable quantities on the stream bed. This size fraction is called wash load (*35*) because it does not interact significantly with the stream bed nor depend on local hydraulics. When developing physical relations for total sediment load, wash load is excluded (*36*). The fraction of sediment that interacts with the stream bed is known as the bed material load. The cutoff grain size for wash load is inferred based on the bed GSD, and a size of D_5 or D_{10} (sediment size at which 5 or 10% of the distribution is finer) has been considered in the past (*37*, *38*). This value varies among rivers systems, although conventionally, the sand-silt transition (that is, 62.5 μm) is used as a rule of thumb for many sand-bed rivers (*39*). However, the Huanghe has a fine-grained bed with a median diameter near this value (62.5 μm). Hence, an alternative value for the wash load/bed material load cutoff size is inferred based on the standard criterion whereby the cutoff is established as the D_5 size (*37*); using the GSDs of the bed material and suspended sediment from six stations on the lower Huanghe, this value is estimated to be 15 μm (Fig. 1B). A sensitivity analysis shows that the results shown below are insensitive to the cutoff grain size within a fairly broad range (see Supplementary text).

EH considers energy conservation for a unit fluid column of sediment-laden flow moving along the stoss face of a wavy bedform (for example, a dune) (fig. S3) (*33*). The energy required to elevate the column (per unit time) from trough to crest is $\rho RgCHUH_b/L_b$, where ρ is the water density and H_b and L_b are the wave height and wavelength, respectively. The driving power is related to the product of the sediment driving force, $\tau_{sf} - \tau_c$, and bed shear velocity, $U^* = \sqrt{\tau/\rho}$, where τ_{sf} is the bed shear stress due to skin friction, τ_{fd} is the bed shear stress due to bedform form drag, τ_c is

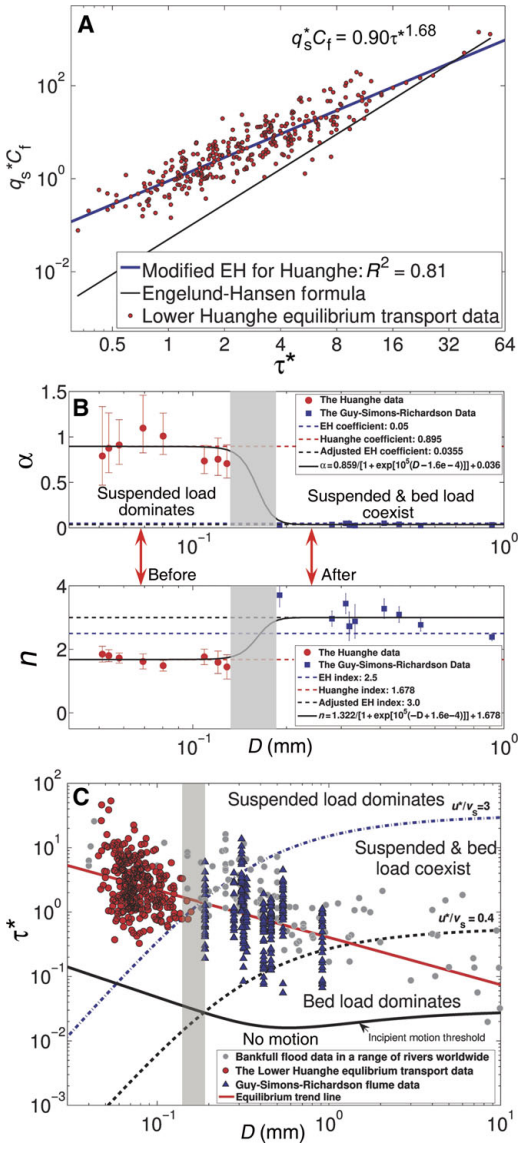

Fig. 2. GEH formula for the lower Huanghe sediment transport data and the universal formula for both fine-grained and sandy environments. (**A**) Data from the lower Huanghe collapse to a power law relation, similar to the EH formula, but with a significantly different coefficient α and power *n*. Note that the sediment transport rate in the lower Huanghe is about 15 times larger than that predicted by the original EH formula. (**B**) The coefficient α and the power *n* of GEH show an abrupt transition (light brown bar) as the grain size of bed material transits through the range of 130 to 190 μm. The error ranges denote the 95% confidence intervals for α and *n*. The complete form of the universal sediment transport relation can be found in Supplementary text. The red arrows show the median bed material grain sizes at Huayuankou (150 km downstream of Xiaolangdi Dam; see fig. S1) before and after the Xiaolangdi Dam construction. In addition to the dependence on grain size, the coefficient α and the power *n* may also have a weak dependence on Fr (see fig. S6). The adjusted values of coefficient α and the power *n* are based on the complete Guy-Simons-Richardson database (see Materials and Methods). (**C**) The grain size range where the abrupt transition (light brown bar) is seen coincides with the transition of sediment transport modes; within the grain size range of 130 to 190 μm, the sediment transport mode transitions from a range where the suspended load is dominant to a range where the substantial suspended load and bed load coexist. The black dashed line denotes the threshold of bed load dominance (u^*/v_s = 0.4), and the blue broken line denotes the threshold of suspended load dominance (u^*/v_s = 3). Here, u^* is the shear velocity, and v_s is the settling velocity of a sediment particle.

the critical shear stress, and $\tau = \tau_{sf} + \tau_{fd}$. In addition, the total shear stress is $\tau = \rho gHS = \rho C_f U^2$ in steady and uniform flow. In regard to the two types of bed stress, skin friction stress is the driving force for sediment transport, whereas form drag stress represents resistance to flow produced by topographic irregularities of the channel and is considered to contribute little to sediment transport. Energy conservation thus dictates $\rho R g q_s H_b / L_b = e(\tau_{sf} - \tau_c)U^*$, where *e* is an efficiency parameter.

Nondimensionalizing to the respective Einstein and Shields numbers, $q_s^* = q_s/\sqrt{RgD_g^3}$ and $\tau^* = \tau/(R\rho g D_g)$, we obtain

$$C_f q_s^* = eC_f L_b/H_b \times (\tau_{sf}^* - \tau_c^*)\sqrt{\tau^*} \quad (1)$$

EH found that $C_f L_b/H_b$ takes the constant value 0.235 and that the relation between skin friction shear stress and total shear stress is $\tau_{sf}^* - \tau_c^* = 0.4\tau^{*2}$ for a dune-covered bed. Calibration with flume data yielded e = 0.532, giving the original EH relation $C_f q_s^* = \alpha_{EH}\tau^{*5/2}$. We hypothesize that the discrepancy between measured and predicted sediment transport (Fig. 2A) could be due to differences in bedform characteristics between the Huanghe and other sand-bed rivers.

EH is based on energy conservation, so the underlying physics can be generalized, whereby the form of the resistance relation (Eqs. 2A and 2B) is used to close Eq. 3

$$\tau_{sf}^* - \tau_c^* = b\tau^{*n-0.5} \quad (2A)$$

$$\alpha = ebC_f L_b/H_b \quad (2B)$$

Here, α is the coefficient, and *n* is the exponent of the generalized EH (GEH) formula. Note that *n* is also contained in the resistance relation (n − 0.5). Substituting Eqs. 2A and 2B into Eq. 1

$$C_f q_s^* = \alpha\tau^{*n} \quad (3)$$

The fact that Eqs. 2A and 3 include the same exponent *n* underlines the importance of the resistance relation (Eq. 2A) in setting sediment transport capacity (*40*). Here, both α and *n* are strongly related to the bed state, namely, the presence and geometry of bedforms. A resistance diagram consisting of a plot of τ^* versus τ_{sf}^* in the original EH exposition shows that when $n \geq 2.0$, $n = 1.5$, and $n < 1.5$, the bed state corresponds to dunes, upper plane bed, and antidunes, respectively (*33*). In Eq. 2B, the aspect ratio L_b/H_b varies greatly from plane bed to dune regime, whereas e, b, and C_f vary less.

The nondimensional numbers $C_f q_s^*$ and τ^* yield a good power law relation (similarity collapse) (Fig. 2A), indicating that the GEH accurately describes measured Huanghe sediment flux values; the coefficient and power index values are $\alpha = 0.90 = 18\alpha_{EH}$ and $n = 1.68$, respectively. The difference can be seen in Fig. 2B, wherein we compare the parameters for the Huanghe database with the Guy-Simons-Richardson database (*41*), which was used to develop the original EH formula.

The coefficient α and power *n* show abrupt transitions when the bed material grain size varies through the range of 130 to 190 μm. Recalling that $\alpha = ebC_f L_b/H_b$ and that e, b, and C_f are weakly varying coefficients, the large ratio $\alpha/\alpha_{EH} = 18$ indicates that L_b/H_b is an order of magnitude larger in the Huanghe than other sand-bed rivers, implying very low amplitude bedform features (dunes). The value $n = 1.68$ is close to the value for upper-regime plane bed ($n = 1.5$), suggesting the presence

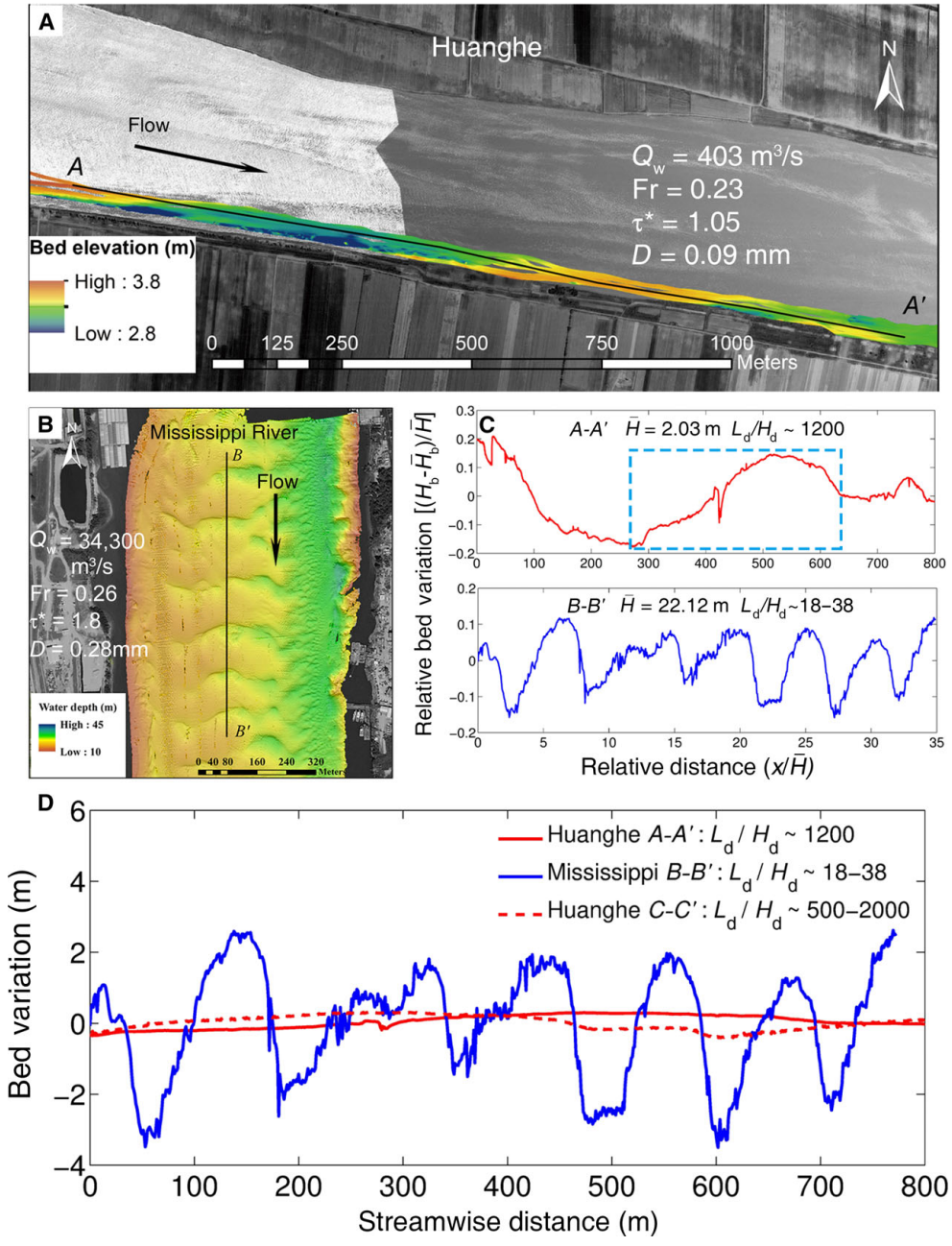

Fig. 3. Channel bed bathymetry data of the lower Huanghe and lower Mississippi River. (**A**) Bathymetric map of a straight reach of the lower Huanghe surveyed during the base flow period of 2016 (*A*-*A*′). (**B**) Bathymetric map of a straight reach of the lower Mississippi River (*B*-*B*′). (**C**) Relative bed variation along two longitudinal profiles, where *x* is the downstream distance from the survey origin point, H_b is the bed elevation, $\bar{H}_b$ is the average bed elevation, $\bar{H}$ is the average water depth, and L_d and H_d are the wavelength and wave height of dunes, respectively. (**D**) Comparison of long profiles of bed elevation between the Huanghe and the Mississippi River, illustrating the difference in bedform morphology. The *A*-*A*′ segment of the Huanghe bed profile shown here is taken from the zone defined by the blue rectangle in (C), whereas the *C*-*C*′ segment of Huanghe profile is taken from fig. S7B and corresponds to the flood season period of WSRS in 2015.

of long-crested bedforms (dunes) approaching upper-regime plane bed in the Huanghe. Thus, form drag can be neglected, with $\tau^*_{fd} \approx 0$ and $\tau^*_{sf} \approx \tau^*$. Both parameters therefore suggest that the phase transition of sediment load described above is associated with change in the state of bed morphology and, specifically, bedform size. This theoretical prediction is verified independently by comparing τ^*_{sf} with τ^* (see Supplementary text).

The relative absence of dunes in the lower Huanghe has been previously inferred (*42*, *43*), but direct supporting evidence is sparse. Here, we provide documentation of dune size in the Huanghe using the recently acquired multibeam bathymetry data collected near Lijin during the flood period of 2015 WSRS (fig. S7) and base-flow period of 2016 (Fig. 3). Prevailing flow conditions facilitated dune development [that is, Froude number (Fr), ~0.23 to 0.5] (*44*), with the aspect ratio L_b/H_b ranging from 500 to 2000 (1200 for base flow and 500 to 2000 for flood flow). These values are significantly larger than measurements from natural rivers and flume experiments with sand beds, where the aspect

ratio ranges from 10 to 100 (*45*, *46*). As an example, dunes measured in the lower Mississippi River have aspect ratios of 18 to 38, that is, close to those predicted by the standard EH. Therefore, both measurements and predictions indicate that the Huanghe has bedforms (dunes) with aspect ratios that are an order of magnitude larger than most large sand-bed rivers. We speculate that the form of these dunes is due to the fine sand–silt material of the Huanghe bed because this sediment size has a long particle advection length (*47*) and moves mostly in suspended load, whereas the mixture of bed load and suspended load over a typical sand bed is more conducive to interacting with bedforms that scale with the depth, such as standard dunes (Fig. 2C). This point merits further study, and a stability analysis of bedforms on fine-grained beds could potentially provide additional insight.

The present universal GEH formula agrees well with both the lower Huanghe sediment database and the Guy-Simons-Richardson database (Fig. 4); notably, the universal GEH formula can predict the dimensionless sediment flux over 10 orders of magnitude, covering characteristic bed material grain size from 15 μm to 1 mm. The performance of the GEH formulation for the fine-grained rivers is also compared to three other relations designed for sediment transport in the Huanghe (see Supplementary text and table S3). Of the four relations, only the GEH is based on a known value of bed material size; the others require the circularity of prior knowledge about the suspended sediment GSD to predict transport rates.

DISCUSSION AND CONCLUSIONS

The exceptionally high sediment transport rate measured for the lower Huanghe has a physical basis: Bedforms with large aspect ratios reduce form drag, and thus, boundary shear stress can be nearly entirely used for sediment transport. It can be expected that results from the Huanghe can be used to predict the sediment flux in other FGDS, including most of river-coast-marine settings, inland fine-grained rivers, such as Rio Bermejo in Argentina (*48*), Rio Pilcomayo in Argentina and Paraguay (*8*), and the Tarim River in western China (*49*), lahar flows (but with volumetric sediment concentration of less than 5%) (*50*), and subglacial water-sediment systems (*51*, *52*). The new transport formula can not only help meet the rapidly emerging need to understand the dynamics of fine-grained sediment transport but also be applied universally to a wide range of sediment dispersal systems with both silt and coarser-grained sandy beds.

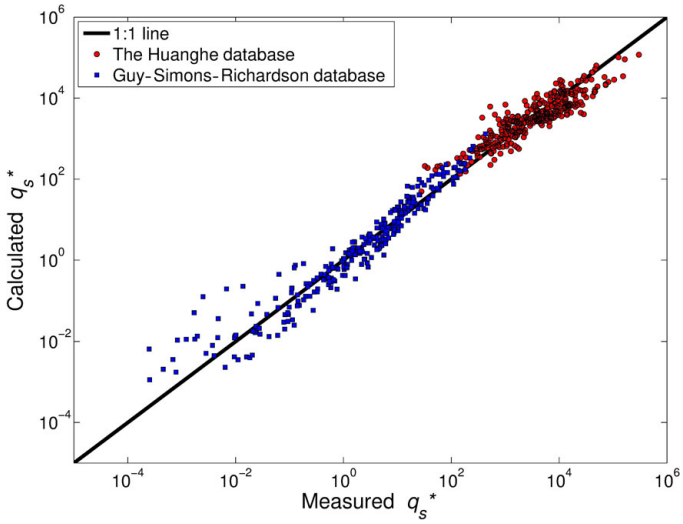

Fig. 4. Comparisons between the calculated dimensionless sediment flux based on the universal GEH formulation and data from two databases.

The analyses presented here indicate that a sediment load phase transition arises at the grain size range of 130 to 190 μm. This finding has important implications for evaluating the environmental impacts of fluvial dam construction and removal. For example, the engineered WSRS on the Huanghe has led to channel degradation and coarsening of the bed material (from ~70 to 250 μm; Fig. 2B) for the upper reaches of the lower Huanghe, just below the Xiaolongdi dam. The formula presented here indicates that this will lower sediment transport efficiency by an order of magnitude; in addition, the added drag produced by dunes with a lower aspect ratio could increase water stage. If this effect exceeds degradation, it could leave the system prone to levee overtopping during flood events. This unintended consequence of the WSRS is worth noting because it could cause a catastrophic failure of river levees during floods. These consequences may be unique to the case of the Huanghe. However, more generally, during dam removal or reservoir sluicing, sediment discharge could rapidly increase due to bed material fining via the inflow and temporary deposition of fine-grained sediment from the impoundment (*6*, *7*). This would produce a local increase in the elevation of the downstream channel bed and floodplain, further enhancing flood potential. The sediment transport formula presented here is applicable to nearly the full range of lowland rivers. The impact of constructing or removing a dam in terms of sediment transport and subsequent stability of the channel may be evaluated with our new sediment transport relation and previous knowledge of the GSD of bed sediment.

MATERIALS AND METHODS

Original form of EH formula

The EH formula is a total load equation, comprising both the bed material part of suspended load and the bed load. Its dimensionless form reads $C_f q_s^* = \alpha_{EH} \tau^{*5/2}$, where $q_s^* = q_s / \sqrt{RgD^3}$ is the dimensionless sediment discharge, that is, the Einstein number [$q_s = HUC$ is the sediment discharge per unit width (H is the water depth; U is the average flow velocity; and C is the volumetric sediment concentration, with contributions from both the bed material part of suspended load and the bed load); R is the sediment submerged specific gravity (1.65 for quartz); g is the gravitational acceleration; and D is the characteristic (nominal) grain size of bed material], and $\alpha_{EH} = 0.05$. In addition, $\tau^* = \tau/(\rho gRD)$ is the dimensionless form of total shear stress, that is, the Shields number, where $\tau = \rho C_f U^2 = \rho u^{*2}$ is the total shear stress (C_f is the bed resistance coefficient and u^* is the shear velocity). For the normal flow condition (steady and uniform flow), $\tau = \rho gHS$, where S is the channel bed slope, so $\tau^* = HS/(RD)$ and $C_f = gHS/U^2$.

While developing the original form of the formula, Engelund and Hansen (*33*) used only four of the nine groups of data in the Guy-Simons-Richardson database (*41*), obtaining a coefficient $\alpha_{EH} = 0.05$ and power index $n_{EH} = 2.5$. Here, all nine groups of data in the Guy-Simons-Richardson database (*41*) are used, and the adjusted values for α and n were determined to be 0.0355 and 3.0, respectively. The adjusted formula had only a slight difference from the original form in terms of predictive accuracy.

Quasi-equilibrium sediment transport database

Measurements of sediment load were collected at hydrological stations along the Huanghe since the 1950s. During sampling, several positions

were located equally along a cross section, where three to five vertical sediment samples were collected. The vertical velocity profile, water discharge, water surface level, and surface gradient were also measured. The sediment concentration and GSDs of sediment samples (from both the water column and the bed) were subsequently analyzed; the grain size resolution was 5 μm. The sediment load data used here pertain to total load, which comprises the measured suspended load and a correction with the modified Einstein procedure (MEP) to account for the bed load. Because the measurement of both suspended sediment concentration and velocity extended down to a reference height not far above the bed, the MEP was used to calculate the bed load concentration and velocity below the reference height. On the basis of a theoretical model, the calculated bed load flux was added to the total sediment load. Additional details of this procedure were found in the study of Colby and Hembree (*53*). However, it should be pointed out that the component of bed load in the Huanghe was negligible. The average sediment concentration C and velocity U used here were the cross-sectional flux-averaged bed material load concentration and cross-sectionally averaged velocity, respectively.

The quasi-equilibrium database used here was selected from routine data collected during the 1980s, for which bed material GSDs are available, and before the construction of the Xiaolangdi Dam and reservoir. The criteria for data selection were that (i) water discharges and water surface level remain unchanged before and after the two-hour survey (steady flow) and (ii) the suspended load is consistent with other measurements at the same water discharge, surveyed at other times (*19*, *54*). The quasi-equilibrium data covered a large range of flow and grain size conditions. Water depth ranged from 0.55 to 7.8 m, flow velocity ranged from 0.39 to 2.90 m/s, water surface slope ranged from 2×10^{-5} to 9×10^{-4}, and the geometric mean grain size of bed material ranged from 15 to 158 μm. Therefore, the database well characterized the flow and bed material conditions during both nonflood and flood seasons.

Bed bathymetry data

The survey cruises of the lower Huanghe were conducted during the WSRS of 2015 and the nonflood (base flow) season of 2016. The survey site was at Kenli, near Dongying, China, close to Lijin Hydrological Station and 83 km upstream of the outlet. The bathymetric data were collected from a boat following a straight reach. The acquisition and processing procedures followed that of Nittrouer *et al.* (*55*). Because of the relatively shallow depth of the Huanghe compared to the Mississippi River, the multibeam survey swath width was considerably narrower, because this width is proportional to water depth beneath the multibeam head; for the Huanghe, this depth was 1.0 to 4.0 m during the survey, whereas for the Mississippi River, it was 20 to 40 m.

SUPPLEMENTARY MATERIALS

Supplementary material for this article is available at http://advances.sciencemag.org/cgi/content/full/3/5/e1603114/DC1

Supplementary text

table S1. Summary of hydraulic and grain size conditions of databases that were used for the development and validation of previous and present formulae.

table S2. Sensitivity analysis of the GEH formulation to cutoff grain size.

table S3. Comparisons between computed and measured sediment discharge in the Huanghe.

fig. S1. Map of the Huanghe Basin and the Loess Plateau.

fig. S2. Sediment concentration diagram.

fig. S3. Schematic diagram of hydrodynamics over asymmetrical, angle-of-repose dunes.

fig. S4. The lower Huanghe data and GEH formulae.

fig. S5. Comparison between the Shields number due to skin friction and the Shields number due to boundary shear stress at Huayuankou and Lijin gauging stations, respectively.

fig. S6. Dependence of the coefficient α and the power index n of the GEH on Fr.

fig. S7. Channel bed bathymetry data of the lower Huanghe during the flood period of the 2015 WSRS.

References (*56*–*68*)

REFERENCES AND NOTES

1. S. Tulaczyk, B. Kamb, R. P. Scherer, H. F. Engelhardt, Sedimentary processes at the base of a West Antarctic ice stream: Constraints from textural and compositional properties of subglacial debris. *J. Sediment. Res.* **68**, 487–496 (1998).
2. G. S. Visher, Grain size distributions and depositional processes. *J. Sediment. Res.* **39**, 1074–1106 (1969).
3. J.-B. W. Stuut, M. A. Prins, R. R. Schneider, G. J. Weltje, J. H. F. Jansen, G. Postma, A 300-kyr record of aridity and wind strength in southwestern Africa: Inferences from grain-size distributions of sediments on Walvis Ridge, SE Atlantic. *Mar. Geol.* **180**, 221–233 (2002).
4. D. Sun, J. Bloemendal, D. K. Rea, J. Vandenberghe, F. Jiang, Z. An, R. Su, Grain-size distribution function of polymodal sediments in hydraulic and aeolian environments, and numerical partitioning of the sedimentary components. *Sediment. Geol.* **152**, 263–277 (2002).
5. S. W. Ruff, P. R. Christensen, Bright and dark regions on Mars: Particle size and mineralogical characteristics based on Thermal Emission Spectrometer data. *J. Geophys. Res. Planets* **107**, 2-1–2-22 (2002).
6. J. A. Warrick, J. A. Bountry, A. E. East, C. S. Magirl, T. J. Randle, G. Gelfenbaum, A. C. Ritchie, G. R. Pess, V. Leung, J. J. Duda, Large-scale dam removal on the Elwha River, Washington, USA: Source-to-sink sediment budget and synthesis. *Geomorphology* **246**, 729–750 (2015).
7. J. E. O'Connor, J. J. Duda, G. E. Grant, 1000 dams down and counting. *Science* **348**, 496–497 (2015).
8. J. P. Martín-Vide, M. Amarilla, F. J. Zárate, Collapse of the Pilcomayo River. *Geomorphology* **205**, 155–163 (2014).
9. J. P. M. Syvitski, C. J. Vörösmarty, A. J. Kettner, P. Green, Impact of humans on the flux of terrestrial sediment to the global coastal ocean. *Science* **308**, 376–380 (2005).
10. J. E. Cohen, C. Small, A. Mellinger, J. Gallup, J. Sachs, Estimates of coastal populations. *Science* **278**, 1209–1213 (1997).
11. A. A. Kalinske, C. H. Hsia, *Study of Transportation of Fine Sediment by Flowing Water* (Bulletin 29, University of Iowa Studies in Engineering, University of Iowa, 1945).
12. V. A. Vanoni, N. H. Brooks, "Laboratory studies of the roughness and suspended load of alluvial streams" (Report no. E-68, Sedimentation Laboratory, California Institute of Technology, 1957).
13. E. M. Laursen, The total sediment load of streams. *J. Hydraul. Div.* **84**, 1530–1536 (1958).
14. J. C. Willis, N. L. Coleman, W. M. Ellis, Laboratory study of transport of fine sand. *J. Hydraul. Div.* **98**, 489–501 (1972).
15. S. Wang, R. Zhang, Experimental study on transport rate of graded sediment, in *Proceedings of the International Conference on River Flood Hydraulics*, W. R. White, Ed. (John Wiley & Sons Ltd., 1990), pp. 299–306.
16. S. Wang, Y. Cheng, Y. Hui, A study on the transport capacity of nonuniform sediment in open channels. *J. Hydraul. Eng.* **1**, 1–9 (1998).
17. W. R. Brownlie, N. H. Brooks, "Prediction of flow depth and sediment discharge in open channels" (California Institute of Technology, 1982).
18. B. Wu, D. S. van Maren, L. Li, Predictability of sediment transport in the Yellow River using selected transport formulas. *Int. J. Sediment Res.* **23**, 283–298 (2008).
19. Y. F. Zhang, Y. Q. Long, G. Q. Shen, Adaptability of sediment transport formula to the Yellow River, in *Proceedings of the 7th International Symposium on River Sedimentation* (Taylor & Francis, 1998), pp. 87–92.
20. B. Wu, G. Wang, J. Ma, R. Zhang, Case study: River training and its effects on fluvial processes in the lower Yellow River, China. *J. Hydraul. Eng.* **131**, 85–96 (2005).
21. Wuhan University on Hydraulic and Electrical Engineering and China Institute of Water Resources and Hydropower Research, *China History of Water Conservancy* (China Water Power Press, 1985).
22. Q. Wu, Z. Zhao, L. Liu, D. E. Granger, H. Wang, D. J. Cohen, X. Wu, M. Ye, O. Bar-Yosef, B. Lu, J. Zhang, P. Zhang, D. Yuan, W. Qi, L. Cai, S. Bai, Outburst flood at 1920 BCE supports historicity of China's Great Flood and the Xia dynasty. *Science* **353**, 579–582 (2016).
23. J. D. Milliman, R. H. Meade, World-wide delivery of river sediment to the oceans. *J. Geol.* **91**, 1–21 (1983).
24. G. J. Orton, H. Reading, Variability of deltaic processes in terms of sediment supply, with particular emphasis on grain size. *Sedimentology* **40**, 475–512 (1993).
25. S. Wang, B. Fu, S. Piao, Y. Lü, P. Ciais, X. Feng, Y. Wang, Reduced sediment transport in the Yellow River due to anthropogenic changes. *Nat. Geosci.* **9**, 38–41 (2016).

26. Y. Saito, Z. Yang, K. Hori, The Huanghe (Yellow River) and Changjiang (Yangtze River) deltas: A review on their characteristics, evolution and sediment discharge during the Holocene. *Geomorphology* **41**, 219–231 (2001).
27. R. Slingerland, N. D. Smith, River avulsions and their deposits. *Annu. Rev. Earth Planet. Sci.* **32**, 257–285 (2004).
28. Y. Chen, I. Overeem, A. J. Kettner, S. Gao, J. P. M. Syvitski, Modeling flood dynamics along the superelevated channel belt of the Yellow River over the last 3000 years. *J. Geophys. Res. Earth Surf.* **120**, 1321–1351 (2015).
29. V. Ganti, Z. Chu, M. P. Lamb, J. A. Nittrouer, G. Parker, Testing morphodynamic controls on the location and frequency of river avulsions on fans versus deltas: Huanghe (Yellow River), China. *Geophys. Res. Lett.* **41**, 7882–7890 (2014).
30. Y. Yongguia, S. Xuefa, W. Houjie, Y. Chengkun, C. Shenliang, L. Yanguang, H. Limin, Q. Shuqing, Effects of dams on water and sediment delivery to the sea by the Huanghe (Yellow River): The special role of Water-Sediment Modulation. *Anthropocene* **3**, 72–82 (2013).
31. J.-g. Chen, W.-h. Zhou, P. Sun, Effects of water-sediment regulation by Xiaolangdi Reservoir on channel erosion in the Lower Yellow River. *J. Sediment Res.* **3**, 1–7 (2009).
32. H. Wang, N. Bi, Y. Saito, Y. Wang, X. Sun, J. Zhang, Z. Yang, Recent changes in sediment delivery by the Huanghe (Yellow River) to the sea: Causes and environmental implications in its estuary. *J. Hydrol.* **391**, 302–313 (2010).
33. F. Engelund, E. Hansen, *A Monograph on Sediment Transport in Alluvial Streams* (Tekniskforlag Skelbrekgade 4 Copenhagen V, 1967).
34. G. V. Wilkerson, G. Parker, Physical basis for quasi-universal relationships describing bankfull hydraulic geometry of sand-bed rivers. *J. Hydraul. Eng.* **137**, 739–753 (2010).
35. E. W. Lane, Report of the subcommittee on sediment terminology. *Trans. Am. Geophys. Union* **28**, 936–938 (1947).
36. H. A. Einstein, N. Chien, Can the rate of wash load be predicted from the bed-load function? *Trans. Am. Geophys. Union* **34**, 876–882 (1953).
37. N. Chien, Z. Wan, *Mechanics of Sediment Transport* (American Society of Civil Engineers, 1999).
38. H. A. Einstein, *The Bed-Load Function for Sediment Transportation in Open Channel Flows* (U.S. Department of Agriculture, 1950).
39. National Research Council, *River Science at the U.S. Geological Survey* (National Academies Press, 2007).
40. G. Parker, A. G. Anderson, Basic principles of river hydraulics. *J. Hydraul. Div.* **103**, 1077–1087 (1977).
41. H. P. Guy, D. B. Simons, E. V. Richardson, "Summary of Alluvial Channel Data From Flume Experiments, 1956-61" (U.S. Geological Survey Professional Paper 462–I, U.S. Government Printing Office, 1966).
42. J. H. Van den Berg, A. van Gelder, A new bedform stability diagram, with emphasis on the transition of ripples to plane bed in flows over fine sand and silt. *Spec. Publ. Int. Assoc. Sediment.* **17**, 11–21 (1993).
43. N. Qian, W. H. Zhou, *Alluvial Process of the Lower Yellow River* (Science Press, 1965).
44. M. Colombini, Revisiting the linear theory of sand dune formation. *J. Fluid Mech.* **502**, 1–16 (2004).
45. J. Best, The fluid dynamics of river dunes: A review and some future research directions. *J. Geophys. Res.* **110**, F04S02 (2005).
46. S. Naqshband, J. S. Ribberink, S. J. M. H. Hulscher, Using both free surface effect and sediment transport mode parameters in defining the morphology of river dunes and their evolution to upper stage plane beds. *J. Hydraul. Eng.* **140**, 06014010 (2014).
47. V. Ganti, M. P. Lamb, B. McElroy, Quantitative bounds on morphodynamics and implications for reading the sedimentary record. *Nat. Commun.* **5**, 3298 (2014).
48. G. H. Sambrook Smith, J. L. Best, J. Z. Leroy, O. Orfeo, The alluvial architecture of a suspended sediment dominated meandering river: The Río Bermejo, Argentina. *Sedimentology* **63**, 1187–1208 (2016).
49. Q. Feng, Z. Li, G. Cheng, Grain size characteristics of sedimentary and the climatic change in middle reaches of Tarim River. *Acta Sed. Sinica* **14**, 227–233 (1996).
50. J. Bohannon, Stalking a volcanic torrent. *Science* **316**, 1562–1563 (2007).
51. H. A. Fricker, T. Scambos, R. Bindschadler, L. Padman, An active subglacial water system in West Antarctica mapped from space. *Science* **315**, 1544–1548 (2007).
52. A. M. Smith, T. Murray, K. W. Nicholls, K. Makinson, G. Aðalgeirsdóttir, A. E. Behar, D. G. Vaughan, Rapid erosion, drumlin formation, and changing hydrology beneath an Antarctic ice stream. *Geology* **35**, 127–130 (2007).
53. B. R. Colby, C. H. Hembree, *Computations of Total Sediment Discharge, Niobrara River Near Cody, Nebraska* (U.S. Geological Survey, 1955).
54. Y. Q. Long, Y. F. Zhang, Study on the Yellow River sediment from the viewpoint of total sediment. *Yellow River* **24**, 28–29 (2002).
55. J. A. Nittrouer, M. A. Allison, R. Campanella, Bedform transport rates for the lowermost Mississippi River. *J. Geophys. Res.* **113**, F03004 (2008).
56. M. H. Garcia, *Sedimentation Engineering: Processes, Measurements, Modeling, and Practice* (American Society of Civil Engineers, 2008).
57. J. A. Nittrouer, D. Mohrig, M. Allison, Punctuated sand transport in the lowermost Mississippi River. *J. Geophys. Res.* **116**, F04025 (2011).
58. C. T. Yang, A. Molinas, B. Wu, Sediment transport in the Yellow River. *J. Hydraul. Eng.* **122**, 237–244 (1996).
59. B. S. Wu, Y. Q. Long, Several modifications for sediment transport capacity formulas of the Yellow River. *Yellow River* **95**, 1–4 (1993).
60. R. J. Zhang, A study of the sediment transport capacity of the middle and lower Yangtze River. *J. Sediment Res.* **4**, 54–73 (1959).
61. P. Ackers, W. R. White, Sediment transport: New approach and analysis. *J. Hydraul. Div.* **101**, 621–625 (1975).
62. L. C. van Rijn, Sediment transport, part II: Suspended load transport. *J. Hydraul. Eng.* **110**, 1613–1641 (1984).
63. L. C. van Rijn, Unified view of sediment transport by currents and waves. II: Suspended transport. *J. Hydraul. Eng.* **133**, 668–689 (2007).
64. C. T. Yang, Unit stream power equations for total load. *J. Hydrol.* **40**, 123–138 (1979).
65. G. Wang, B. Wu, Z.-Y. Wang, Sedimentation problems and management strategies of Sanmenxia Reservoir, Yellow River, China. *Water Resour. Res.* **41**, W09417 (2005).
66. T. R. Kidder, H. Liu, Bridging theoretical gaps in geoarchaeology: Archaeology, geoarchaeology, and history in the Yellow River valley, China. *Archaeol. Anthropol. Sci.* (**2014**), 1–18 (2014).
67. T. C. Pierson, Hyperconcentrated flow—Transitional process between water flow and debris flow, in *Debris-Flow Hazards and Related Phenomena* (Springer, 2005).
68. J. Xu, Erosion caused by hyperconcentrated flow on the Loess Plateau of China. *Catena* **36**, 1–19 (1999).

Acknowledgments: We thank J. Best, D. Parsons, and M. Lamb for the fruitful discussions. The careful reviews of two anonymous reviewers are greatly appreciated. We thank the survey boat crew from Hydrological Survey Bureau of the Yellow River Mouth and we gratefully acknowledge the field logistical support of Teledyne-RESON, which enhanced our MBES surveys of the Yellow River. **Funding:** H.M., J.A.N., K.N., A.J.M., and G.P. acknowledge the NSF for support through EAR grant no. 1427262, "Coastal SEES Collaborative Research: Morphologic, Socioeconomic, and Engineering Sustainability of Massively Anthropic Coastal Deltas: The Compelling Case of the Huanghe Delta." X.F. acknowledges support from the National Natural Science Foundation of China (NSFC) through grant no. 51525901. Y.Z. acknowledges support from the NSFC through grant no. 51379087. Y.W. acknowledges support from the NSFC through grants no. 51509102 and 5153000441. A.J.M. acknowledges support from the NSF Graduate Research Fellowship under grant no. 145068. **Author contributions:** H.M. designed the study with input from J.A.N., G.P., X.F., Y.Z, and B.W. H.M. wrote the manuscript. J.A.N. and G.P. provided substantial editorial feedback. H.M., K.N., and G.P. performed the sediment transport data analysis. H.M. built up and tested the theoretical model. Y.Z., Y.W., and B.W. selected the historical sediment transport database. H.M., J.A.N., and A.J.M. conducted the field survey, with support from X.F., Y.W., and Y.Z. A.M. processed the multibeam bathymetry data. All authors contributed to the discussion of results and writing of the manuscript. **Competing interests:** The authors declare that they have no competing interests. **Data and materials availability:** All data needed to evaluate the conclusions in the paper are present in the paper and/or the Supplementary Materials. Additional data related to this paper may be requested from the authors.

Submitted 7 December 2016
Accepted 14 March 2017
Published 12 May 2017
10.1126/sciadv.1603114

Citation: H. Ma, J. A. Nittrouer, K. Naito, X. Fu, Y. Zhang, A. J. Moodie, Y. Wang, B. Wu, G. Parker, The exceptional sediment load of fine-grained dispersal systems: Example of the Yellow River, China. *Sci. Adv.* **3**, e1603114 (2017).

ScienceAdvances
AAAS

The exceptional sediment load of fine-grained dispersal systems: Example of the Yellow River, China

Hongbo Ma, Jeffrey A. Nittrouer, Kensuke Naito, Xudong Fu, Yuanfeng Zhang, Andrew J. Moodie, Yuanjian Wang, Baosheng Wu and Gary Parker (May 12, 2017)

Sci Adv 2017, 3:.
doi: 10.1126/sciadv.1603114